Self-organization at finite temperatures of the devil's staircase in Pb/Si(111)

M. Yakes, V. Yeh, M. Hupalo, and M. C. Tringides*
Department of Physics, Iowa State University, Ames, Iowa 50011, USA
(Received 19 December 2003; revised manuscript received 2 March 2004; published 8 June 2004)

The ''devil's staircase'' (DS) is one of the outstanding phase diagrams in physics because it shows a high degree of self-organization driven by a repulsive long-range adatom interaction. An infinite number of phases are predicted to exist which are built hierarchically with simple combinatorial rules. It was found with diffraction and scanning tunneling microscopy that a DS exists in Pb/Si (111) in the range $1.2<\theta<1.33$ monolayers, surprisingly at ~ 120 K, and with phases which extend spatially over macroscopic distances (~ 0.5 mm). The extraordinary amount of atom rearrangement necessary for these phases to form indicates an unexpected degree of self-organization at low temperatures.

DOI: 10.1103/PhysRevB.69.224103 PACS number(s): 61.14.Hg, 64.70.Rh, 68.35.Rh, 68.43.De

I. INTRODUCTION

Surface overlayers provide rich experimental realizations of statistical mechanical predictions related to phase transitions and ordering phenomena in two-dimensional models.[1–4] Temperature vs coverage (T-θ) phase diagrams are normally constructed with the use of different experimental techniques [diffraction, scanning tunneling microscopy (STM), etc.] to map out regions where ordered phases of different symmetry form and to identify the nature of the transition lines separating these regions. A typical phase diagram consists of a finite number of distinct regions for each of the ordered phases present. Although these phases can be highly complex with complicated multicomponent order parameters, they are commonly accounted for in terms of a simple Hamiltonian which includes a set of short-range but possibly competing adatom interactions. The nature of the phase transitions is identified from the temperature or coverage dependence of the order parameter describing the extent of an ordered phase.

Contrary to these expectations based on short-range interactions, a highly unusual phase diagram has been predicted for a system with long range repulsive interactions even in one dimension (1D), i.e., the so called ''devil's staircase'' (DS) phase diagram.[4–8] For example, adatoms on a 1D lattice with coverage θ and interacting with long range repulsion, at $T=0$ form an infinite number of commensurate phases.[9–11] The coverage of each of these phases is in one-to-one correspondence with the denumerable set of rational numbers $\theta=p/q$. The phase with coverage p/q has period q, with the p adatoms occupying sites in unique patterns dictated by the energy minimization of the system. The term ''devil's staircase'' commonly refers to the θ vs $\Delta\mu$ stability curve relating the coverage of a phase to its chemical potential. The stability interval $\Delta\mu$ depends only on the period of the phase q independent of the numerator p. Since rational numbers of arbitrary large denominator can be arbitrarily close to any θ and $\Delta\mu$ decreases with q, the ''staircase'' is built in a piecewise fashion from segments of variable length and has a fractal character well documented in the literature.[12] It has also been shown that an equivalent way to construct the hierarchical patterns of the DS phases is by combining recursively the unit cells of two generating phases of coverage θ_1, θ_2 (which define the coverage limits $\theta_1<\theta<\theta_2$ for the DS). With increasing recursive stages, a larger number of unit cells of the generating phases is used to construct the phase of the higher stage, so its period increases and its stability $\Delta\mu$ decreases.

It has been an outstanding experimental challenge to discover in nature physical realizations of the DS, since physical phenomena are not expected to be described by fractal-like nondifferentiable functions.[13–17] To prove the presence of a DS in a physical system, it is required first to show that a large number of phases are present within a narrow $\Delta\theta$. Second, to show that these phases are generated in the hierarchical way by the same recursive rules used to construct DS phases in the theoretical models.

This challenge is even more demanding when a statistical probe like diffraction (which probes macroscopic distances) is used. The identification of the specific phases from the expected ones based on DS phases is difficult because diffraction spots at new locations emerge as the coverage θ is changed even by minute amounts. For the numerous phases to be identified, it is necessary to prepare within the illuminated area [~ 0.5 mm for spot profile analysis (SPA) low-energy electron diffraction (LEED)] only one or two DS phases, so their characteristic wavevectors can be resolved. The indexing of the spots of even two coexisting phases close in coverage is nontrivial since some of their spots will be difficult to separate. A given DS phase can be conveniently described by the pair (n,m) of integers which denotes the number of unit cells of the generating phases. If the unit vectors of the two generating phases are b_1, b_2 times the substrate lattice constant, then the period of a (n,m) phase is $q=nb_1+mb_2$ and its diffraction spots at $(p/nb_1+mb_2)\%$ fraction of the Brillouin zone (BZ) while a phase with slightly higher coverage $(n-1,\ m)$ has spots at $[p'/(n-1)b_1+mb_2]\%$ BZ. Since p and p' are independent, some spots can be so close that higher resolving power is needed to discern them.

STM directly and unambiguously images the hierarchical DS phases constructed from the two generating phases, but it is more difficult to assess coverage uniformity over macroscopic distances ~ 0.5 mm. However, as demonstrated before,[18] a DS has been discovered in Pb/Si(111) with STM within the range $1.2<\theta<1.333$ monolayers (ML). 12 atomi-

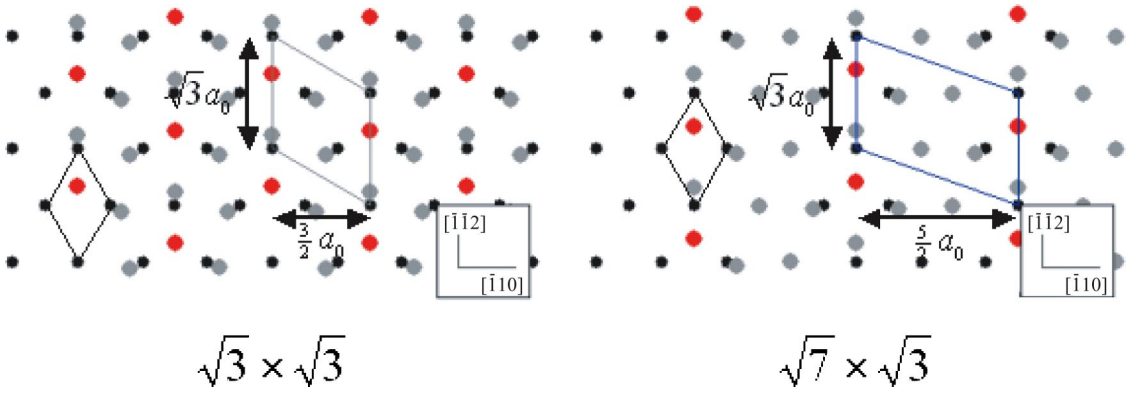

FIG. 1. Schematic illustration of the $\sqrt{3}\times\sqrt{3}$ and $\sqrt{7}\times\sqrt{3}$ unit cell arrangements. Smaller circles denote Si and larger circles Pb atoms. The rows of the 1D structures are aligned along the $[\bar{1}\bar{1}2]$ direction and the DS ordering is along the $[1\bar{1}0]$ direction.

cally resolved phases were identified according to the DS hierarchy. The two generating phases are the $\sqrt{7}\times\sqrt{3}(\theta=1.2$ ML) and $\sqrt{3}\times\sqrt{3}(\theta=1.33$ ML) phases.

However, since the DS phase diagram is strictly speaking valid only at $T=0$, an interesting question is what to expect at finite temperature.[19,20] Not only are the energy differences between the DS phases minute and for phases with larger q less than k_BT, but entropic effects should be taken into account to determine the dependence of the free energy of a phase on temperature. It is not clear how phases of larger q (and lower stability) transform after annealing to higher temperature. Or when the DS phases form after deposition at constant temperature, does the number of the observed phases decrease if higher temperature is used? In either experiment finding out how DS phases transform to each other can be used to deduce their relative stability.

In addition to the question of energetic stability, the transition from one DS phase to another poses questions about the kinetics. High atom mobility is necessary for the surface to rearrange from the initial to the final DS pattern, but it is not clear what is the optimal kinetic pathway for the system to ''discover'' as many DS phases as possible? Intuitively, one expects faster diffusion at higher temperatures to promote the DS formation, since it is easier for the Pb atoms to move to locations dictated by the DS pattern. However, as shown below, quite unexpectedly a DS was discovered at low temperature $\sim$120 K with a large number ($\sim$15) of macroscopically developed phases resolved. This indicates a still poorly understood nonthermal pathway to the highly complex self-organization required by DS. Since the DS phases are close in coverage, inhomogeneities (i.e., of the deposition rate or temperature or surface defects) can potentially limit the spatial extent of the phase. The use of diffraction with $\sim$0.5 mm illuminated area offers the possibility of testing the spatial extent and coverage uniformity. If the coverage has large spatial fluctuations, different DS phases will nucleate and their diffraction patterns will be superimposed, so the spots will smear out. To address all these questions two complementary techniques, high-resolution electron diffraction (SPA LEED) and STM, are employed so the phase structure, kinetics, and spatial distribution can be examined from the atomic to the macroscopic scale.

II. ATOM ARRANGEMENT IN THE DS PHASES

A schematic model of the two generating phases, $\sqrt{3}\times\sqrt{3}$ and $\sqrt{7}\times\sqrt{3}$ is shown in Fig. 1. Smaller circles denote top layer Si atoms, and larger circles denote Pb atoms. The unit cell of the $\sqrt{3}\times\sqrt{3}$ phase has four Pb atoms, three of them are at off-centered $T1$ sites and one atom at the high-symmetry $H3$ site. The unit cell of the $\sqrt{7}\times\sqrt{3}$ phase has six atoms; five of them are at off-centered $T1$ sites and one at the high-symmetry $H3$ site. The coordinates of atoms are obtained from x-ray diffraction experiments[21] and were verified with first principles calculations.[22] Although the long-range stress-driven interaction involves all the Pb atoms within the unit cell, it is a reasonable approximation to assume that an effective interaction exists only between the high-symmetry atoms. The contribution of the Pb atoms at the off-symmetry sites simply renormalizes the strength of

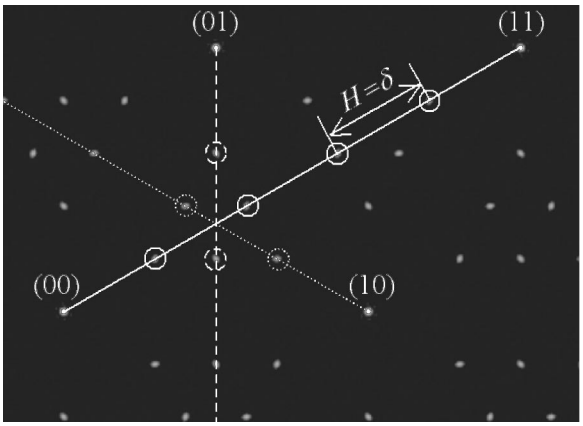

FIG. 2. Schematic representation of the $\sqrt{7}\times\sqrt{3}$ diffraction pattern. Characteristic spots are observed at multiples of 1/5 the diagonal connecting the (00) and (11) spots. Because of the three equivalent $[1\bar{1}0]$ directions which intersect at the (1/3,1/3) position the six spots are arranged in triangular pattern. The triangle height H equals the δ-function separation for this phase.

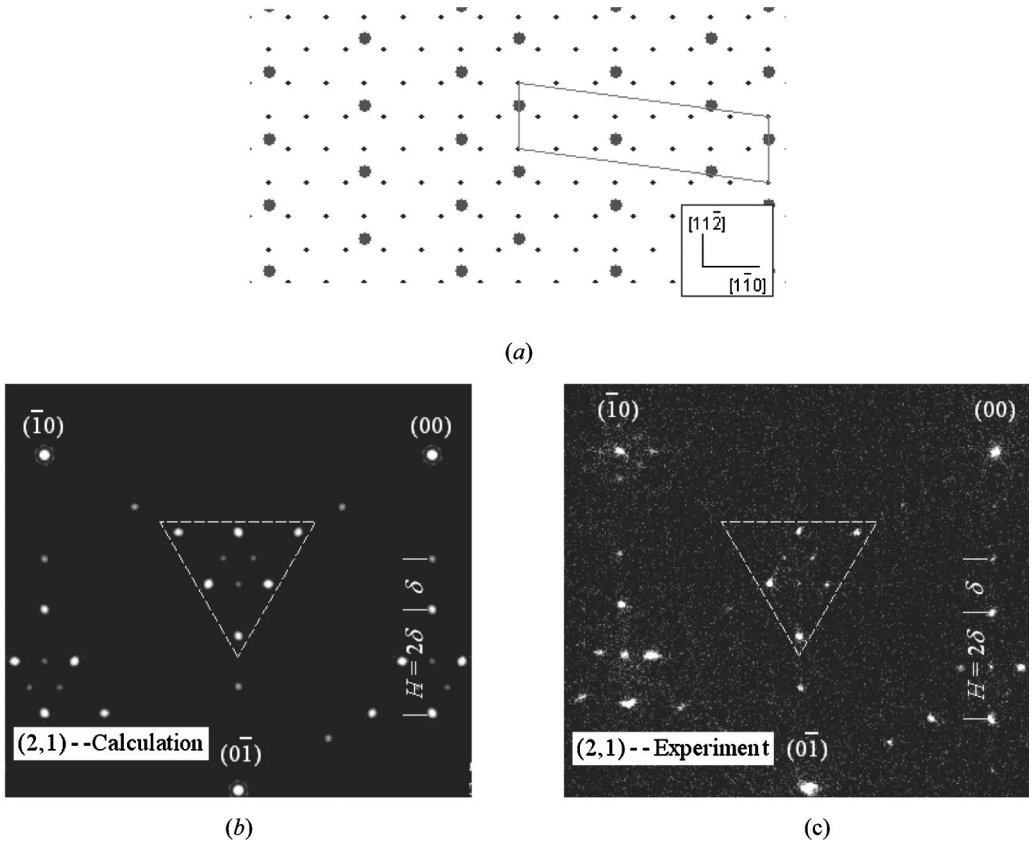

FIG. 3. (a) Schematic representation of the (2,1) phase with the high-symmetry Pb atoms at $H3$-$H3$ positions (b). Kinematically calculated diffraction pattern for the (2,1) phase with only the high-symmetry Pb atoms contributing (c). Experimental pattern for the (2,1) phase showing agreement with the calculated one (except the missing spot at the top vertex of the triangle).

the interaction, but without changing its dependence on r, i.e., the separation between the two interacting atoms. Because of this reason in the kinematic calculations of the diffraction pattern discussed below, only the high-symmetry atoms are assumed in the unit cells.

The diffraction pattern expected for the ideal $\sqrt{3}\times\sqrt{3}$ has superstructure spots located at the (1/3, 1/3) and (2/3, 2/3) positions. The pattern of the $\sqrt{7}\times\sqrt{3}$ phase shown in Fig. 2 has two sets of six superstructure spots arranged on two equilateral triangles centered at the (1/3, 1/3) and (2/3, 2/3) positions. Three of the six spots are at the triangle corners and three are at the center of the opposite sides. The triangle height is 1/5 the separation $4\pi/a_0$ of the (00) and (11) spots (with a_0 the Si lattice constant). The origin of the triangular spot arrangement is related to the threefold symmetry as shown schematically in Fig. 2 because $\sqrt{7}\times\sqrt{3}$ domains can grow in three equivalent directions. The center of the triangle is (1/3,1/3) the intersection of the three equivalent $[1\bar{1}0]$ directions.

An (n,m) DS phase in Pb/Si(111) has unit cell vectors $b_2=\sqrt{3}a_0\vec{y}$, $b_1=\sqrt{3}a_0/2\vec{y}+[(m+n)a_0/2]\vec{x}$ (if $m+n$ is odd) and $b_1=[(m+n)a_0/2]\vec{x}$ (if $m+n$ is even) with period $q=5n+3m$ in units of $a_0/2$. The diffraction pattern resulting from such a phase also has threefold symmetry. It can be expressed as the product of two terms, i.e., the scattering factor within a single (n,m) unit cell $F_{\text{unit cell}}$ times the reciprocal lattice of δ functions originating from long-range order

$$I_{\text{total}}(k_x,k_y)=\left|F_{\text{unit cell}}\sum_{l,s}^{N_x,N_y}\exp(ik_x\cdot lb_1+k_y\cdot sb_2)\right|^2.$$

The δ functions are separated in the $[\overline{1\,10}]$ direction by $\delta=4\pi/a_0/(5n+3m)$. To calculate $F_{\text{unit cell}}$ only the high-symmetry Pb atoms at positions r_s are included

$$F_{\text{unit cell}}=\sum_{s=1}^{s=n+m}\exp(ik_x\cdot r_s).$$

The displacement vector between two neighboring high-symmetry atoms at $H3$-$H3$ sites is $\Delta_{s+1-s}=(3a_0/2,\sqrt{3}a_0/2)$ for neighboring $\sqrt{3}\times\sqrt{3}$ and $\Delta_{s+1-s}=(5a_0/2,\sqrt{3}a_0/2)$ for neighboring $\sqrt{7}\times\sqrt{3}$ unit cells. If there is a shift from an $H3$ to $T4$ position then the second component of Δ_{s+1-s} is 1/3 of the previous shift $\sqrt{3}a_0/6$. Such a small shift can be detected from the ''flipping'' of the triangular pattern and it is related to the formation of other phases (''HIC'', ''SIC'') at higher temperatures not predicted for the DS model and will be discussed in a forthcoming publication.[23]

A typical kinematic calculation of the pattern is shown in Fig. 3 for the (2,1) phase with only $H3$-$H3$ high-symmetry

sites occupied. At the top the real space (2,1) unit cell is shown schematically, i.e., two $\sqrt{7}\times\sqrt{3}$ rows separated by one $\sqrt{3}\times\sqrt{3}$ row. The calculated diffraction pattern is shown to the bottom left and the observed pattern to the bottom right. Spots are expected at $4\pi p/a_0(5n+3m)=p\,\delta$ with p an integer. However not all spots have the same intensity. The δ-function spots closer to the spot of the ideal $\sqrt{7}\times\sqrt{3}$ and the ideal $\sqrt{3}\times\sqrt{3}$ are expected to be the strongest. This suggests that the easiest way to identify an (n,m) phase is to use the triangle height H (i.e., the separation between the most intense spots along $[1\bar{1}0]$). More detailed identification of the phases present can be deduced from 1D scans by determining the integers p, n, m so all spots are matched to $4\pi p/a_0(5n+3m)$.

Next we show how H is related to the phase period for the $(n,1)$ and $(1,m)$ phases, which are the ones observed in the stepwise deposition experiments. For large n the strongest surviving δ-function spots [for the triangle centered at (1/3, 1/3)] are the ones closest to the superstructure spots which are at 1/5 and 2/5, of the diagonal (i.e., $4\pi/a_0=173\%$ BZ where 100% corresponds to the BZ along the $[11\bar{2}]$ direction). This is because $F_{\text{unit cell}}$, which includes mostly $\sqrt{7}\times\sqrt{3}$ unit cells, has broadened superstructure spots at these positions. As θ increases and n decreases, the spacing between the δ-function spots $1/(5n+3)$ increases and they intercept the broadened superstructure spots due to $F_{\text{unit cell}}$ further away from the ideal 1/5 and 2/5 positions. These two intersections form the triangle vertex and the spot at the middle of the opposite side. Their separation is the triangle height H. Since these spots are separated by an integer multiple of the δ-function spacing and are the closest spots to the 1/5 and 2/5 locations of the 173% BZ diagonal, H is the largest possible integer multiple of the δ-function separation which is less than 1/5. This multiple is just n since

$$H/[1/(5n+3)]=\text{int}\left\{\frac{1/5}{1/(5n+3)}\right\}=\text{int}\{n+3/5\}=n,$$

where int{} denotes the integer part of a number.

For the $(1,m)$ phases intense superstructure spots due to $F_{\text{unit cell}}$ are expected closer to the 1/3, 2/3 (in units of the diagonal $4\pi/a_0$ since the $(1,m)$ unit cell has a majority of $\sqrt{3}\times\sqrt{3}$ than $\sqrt{7}\times\sqrt{3}$ unit cells) and should become sharper as m increases. As m decreases the δ-function separation $1/(3m+5)$ is less than 1/3 the separation of the superstructure spots, so the most intense spots closest to the 1/3 spot are simply separated by $1/(3m+5)$ in % BZ which can be used to determine the value of m and identify unambiguously the phase present.

III. FORMATION OF THE DS AT LOW TEMPERATURES

The diffraction experiments were carried out in an UHV system equipped with a SPA LEED diffractometer, an Auger spectrometer, and a mass spectrometer. As described elsewhere, flux calibration was deduced from the Auger breaks at room temperature and low temperatures ~120 K after monolayer completion.[24] In addition, the DS itself provides a fine flux calibration from the relation between the period q of a phase and its coverage $\theta(q)$. The STM experiments were carried in a different UHV system, but under similar preparation conditions (of θ and T).

Different kinetic pathways to prepare the ideal DS were explored. The starting point was a perfect $\sqrt{7}\times\sqrt{3}$ at $T=120$ K. A Pb amount $\Delta\theta<0.1$ ML was added on the $\sqrt{7}\times\sqrt{3}$ followed by thermal annealing; or a larger Pb amount was deposited $\Delta\theta>0.2$ ML and desorbed by heating progressively to higher temperature ~500 K; or the deposition was on a hot surface $T\sim500$ K and at a higher flux rate, so finer coverage control can be obtained when dynamic equilibrium is established between the incident and desorbing atoms. All these recipes rely on the thermal energy of the atoms to generate via diffusion the different (n,m) phases. Although new phases were produced in such thermal preparations with new diffraction spots observed, these were in practically all cases spots corresponding to the most stable DS phases [i.e., the ones with the smaller period $\sqrt{7}\times\sqrt{3}$ (2,1) (1,2) etc.)].

It was surprising that a DS, shown in Fig. 4, with distinct phases (clearly identified from their 1D profiles along the $[1\bar{1}0]$ direction), was prepared at low temperature ~120 K without thermal annealing. The $[1\bar{1}0]$ direction contains the information about DS phases because it corresponds to the direction of ordering of the unit cells $\sqrt{7}\times\sqrt{3}$ and $\sqrt{3}\times\sqrt{3}$ of the generating phases. Each DS phase is prepared after stepwise deposition of only $\Delta\theta\sim0.006$ ML starting initially with the $\sqrt{7}\times\sqrt{3}$ phase on the surface. All 15 phases were observed within ~0.1 ML additional coverage.

A typical 2D pattern is shown in Fig. 3 (bottom right) for the (2,1) phase to be compared to the calculated one (bottom left). The spots are arranged in triangular pattern around the (1/3,1/3) (and the equivalent (2/3,2/3) positions) as expected from the kinematic calculation described in Sec. II. We mostly discuss the triangle around the $(1/3,1/3)$ spot because of better linearity in the SPA LEED optics. The outlined white triangle highlights the triangular pattern of the ideal $\sqrt{7}\times\sqrt{3}$ phase and is used to focus on new spot positions as new DS phases form. One of the six spots in the triangle is missing at the particular energy 80 eV. It is not clear why the spot is absent; possibly it can be due to the dependence of the scattering factor on incident energy or more complex dynamic effects but since it does not affect the identification of the DS phases, this question has not been investigated further.

The 2D patterns for the other DS phases were omitted because of space limitations and because the exact spot positions and wave vector shifts can be measured with better accuracy from the 1D scans along the $[1\bar{1}0]$ direction shown in Fig. 4. Before discussing how the spots were indexed and the DS phases identified, it is easily seen that changes in the pattern occur and new spots at different wave vectors emerge after each 0.006 ML (except the last profile which results after overnight annealing experiment to be discussed below). Numerous phase within narrow $\Delta\theta$ is one of the necessary conditions to realize experimentally a DS. The dotted lines show the wave vectors where the spots of the generating phases are expected as fractions of the diagonal, i.e., its

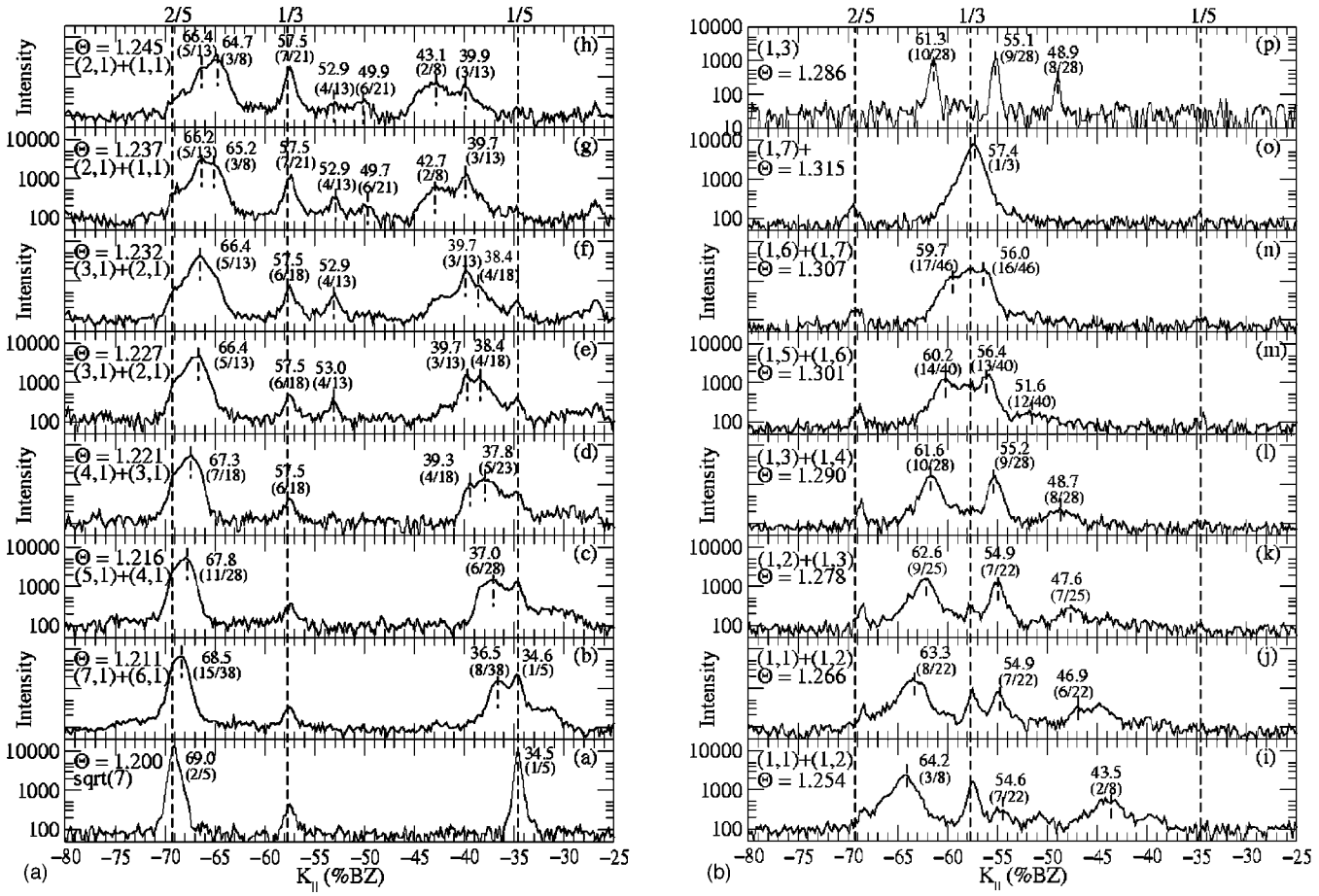

FIG. 4. 1D scans of the low-temperature DS phases formed after stepwise deposition on top of the $\sqrt{7}\times\sqrt{3}$ at 120 K approximately an amount $\Delta\theta\sim 0.006$ ML after each deposition. The phase identified and the average coverage are shown to the left top corner. The dotted lines are at spot positions expected for the ideal $\sqrt{7}\times\sqrt{3}$ [multiples of 1/5 the length of the diagonal (00) and $(\overline{11})$] and the ideal $\sqrt{3}\times\sqrt{3}$ phase (at multiples of 1/3 the diagonal length). The spot position is converted into a fractional ratio which is used to identify the DS phases. For example, 15/38 indicates the presence of the (7,1) phase, 11/28 indicates the presence of the (5,1) phase, etc. Phases with $\theta > 1.25$ ML have 1/2 the expected triangle height H which indicates that $H3$ and $T4$ sites are occupied. The profile p is obtained after overnight annealing of the (1,7) phase $\theta = 1.315$ ML indicating that a single (1,3) phase $\theta = 1.286$ ML occupies the area ~ 0.5 mm illuminated by the electron beam.

length is 173% BZ$=4\pi/a0$) at 1/5 (34.6%), 2/5 (69.3%) for the $\sqrt{7}\times\sqrt{3}$, and at 1/3 (57.3%) for the $\sqrt{3}\times\sqrt{3}$ phase. The shown range in reciprocal space is limited from 25% to 80% of the BZ.

To identify the (DS) phases we first use the height of the triangle H (i.e., the separation between the most intense spots in the 1D scan). In addition we index all the spots which have intensity above twice the background. Some spots overlap either because two majority phases adjacent in coverage cover the illuminated area or because adjacent δ functions of a single phase are within the diffuse spots generated by $F_{\text{unit cell}}$. Both effects result in broader, ''streakier spots'' but clearly the maxima due to the separate components can be resolved and unique wave vectors can be assigned to them. Above a major spot we denote its position as a fraction of the $[1\overline{1}0]$ BZ. For example profile f in Fig. 4(a) has wave vectors at 66.4%, 57.5%, 52.9%, 39.7%, and 38.4%. We search for the fraction closer to the ratio of these wavevectors to the width of the BZ (173%) to assign 5/13, 6/18, 4/13, 3/13, 4/18 to the above wave vectors. This corresponds respectively to the (2,1), (3,1), (2,1), (2,1), and (3,1), phases with (2,1) and (3,1) the main ones. The coverage of an (n,m) phase is $\theta = 1+[(m+n)/(5n+3m)]$. We estimate the coverage on the surface for profile f $\theta = 1.232$ ML from the fractional occupation of the two phases (deduced from their peak intensity) and the additional deposited amount $\Delta\theta\sim 0.006$ ML The profile g in Fig. 4(a) obtained after the next deposition has spots at 66.2%, 65.2%, 57.5%, 52.9%, 49.7%, 42.7%, 39.7% which are identified as 5/13, 3/8, 7/21, 4/13, 6/21, 2/8, 3/13, respectively. The two phases corresponding to the main spots are the (2,1) and (1,1) with average coverage 1.237 ML. In a similar way all the major DS phases and the average coverage have been identified for all 16 profiles of Fig. 4 and are shown to the left corner of each profile.

It is remarkable that in practically all cases only two phases are sufficient to cover more than 95% of the illuminated area of ~ 0.5 mm. However in a few cases, some spots

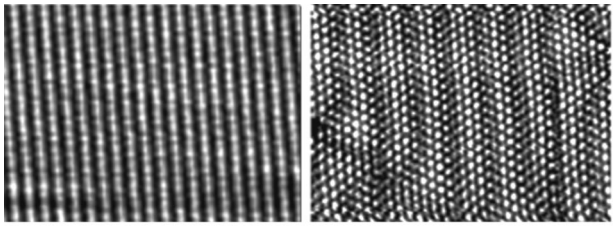

FIG. 5. STM image $18.5\times13.5\ \mathrm{nm}^2$ indicating the formation of a 1D phase (1,2,1,3) $\theta=32/25$ ML after deposition of 0.07 ML on top of the $\sqrt{7}\times\sqrt{3}$ at low temperature $T=40$ K.

which correspond to other phases besides the two major ones are present like spots 57.5% and 49.7% at profile *h* in Fig. 4(a). These spots are accounted for by a second generation phase (3,2) with period 21 [(3,2) should be written more accurately as (1,1,2,1), i.e., one $\sqrt{7}\times\sqrt{3}$, one $\sqrt{3}\times\sqrt{3}$, two $\sqrt{7}\times\sqrt{3}$, one $\sqrt{3}\times\sqrt{3}$ with $\theta=26/21$ slightly less than $\theta=10/8$, the coverage of the (1,1) phase].

For phases with coverage $\theta>1.25$, the observed spots are indexed with height, half the one expected for an (n,m) phase, and the triangularly arranged spots ''flip.'' This indicates that the binding site in the unit cells of the generating phases can be either $H3$ or $T4$ sites, which causes a doubling of the period of an (n,m) phase to $2(5n+3m)$. This in turn implies that the spacing of the δ functions in the $[1\bar{1}0]$ direction is half the spacing for the same (n,m) phase with only $H3$-$H3$ sites occupied. In addition, as mentioned before the shift $\sqrt{3}a_0/6$ between $H3$ and $T4$ sites in the $[11\bar{2}]$ direction is 1/3 the shift between the $H3$ and $H3$ sites. This additional symmetry breaking implies that even fundamental spots (kl) will show satellite spots whenever $\mathrm{mod}_3(k-l)\neq0$. For example, the (00) and (11) spots do not show satellite spots while the (01) and (10) do. These observations, to be discussed in more detail in the future,[23] suggest that the onset of the $H3$-$T4$ occupation is the (1,1) phase.

Phases with higher period q and lower stability, which are not easily observed after thermal annealing, are observed after low-temperature deposition. It is not yet clear why thermal annealing does not lead to these less probable phases, since atom diffusion is faster at higher temperature. However, since the changes of the patterns shown in Fig. 4 are observed immediately after the deposition of $\Delta\theta$, some type of mass transport must be operating very efficiently even at low temperatures, leading to this unusual self-organization. It is intriguing that the readjustment to the next DS phase after

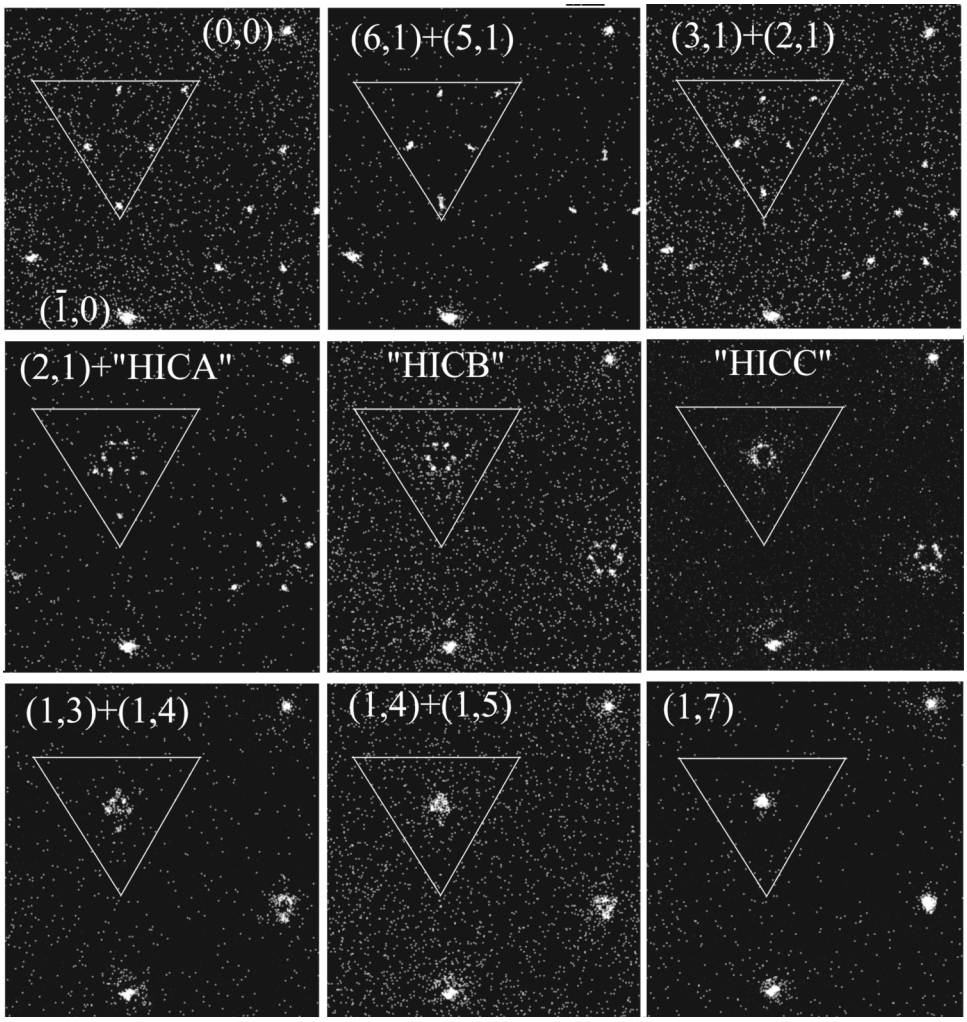

FIG. 6. Stepwise deposition experiments at constant temperature $T=169$ K with $\Delta\theta\sim0.01$ ML showing the formation of 1D phases as expected from the DS hierarchy. In the coverage range $1.23<\theta<1.27$ ML phases of hexagonal symmetry ''HIC'' form.

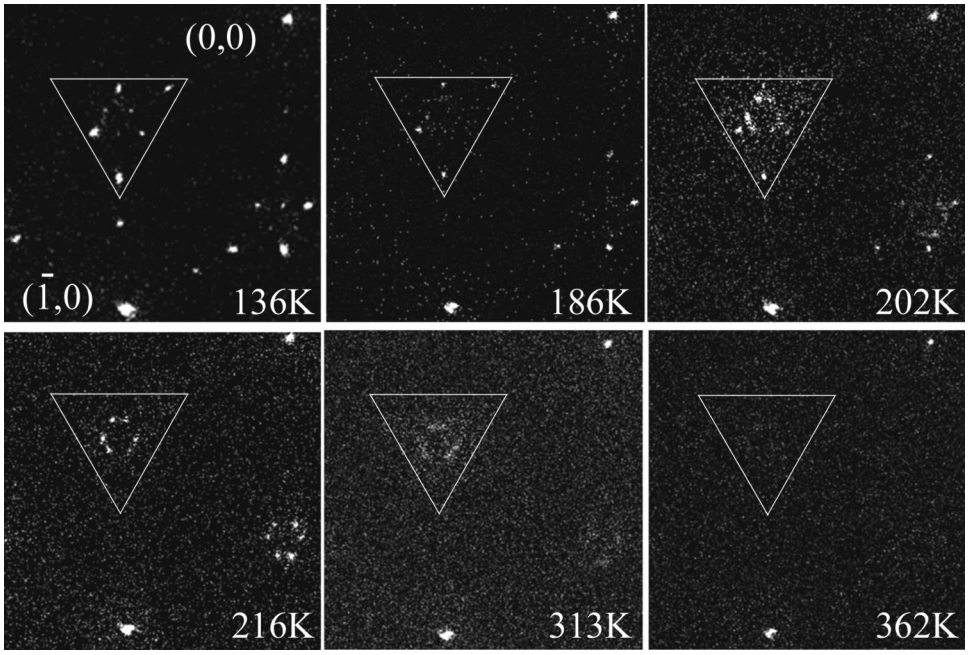

FIG. 7. Thermal annealing of a surface prepared initially in the (2,1) phase $\theta = 1.231$ ML at 136 K showing the progressive evolution to the "HICA" phase (186 K), to the disordered "liquidlike" phase and finally to the (1×1) disordered phase. Cooling the surface back to 136 K recovers the (2,1) phase.

$\Delta\theta$ deposition is very fast ($\sim$few seconds) over the whole macroscopic surface. This is evident from the continuous decrease of the triangle height H with θ seen in the 2D patterns with naked eye and correspondingly in the 1D scans of Fig. 4. The degree of self-organization and highly correlated atom movement which is needed to change at 120 K an initial $(n+1,1)$ to a final $(n,1)$ phase is extensive [since after depositing $\Delta\theta\sim0.006$ ML the average distance between the arriving atoms is $(\Delta\theta)^{-1/2}\sim26a_0$ so atoms need to diffuse at least over this distance to reach their final well-defined positions within the $(n,1)$ unit cell]. The long-range strain interaction between the Pb atoms, which is induced by the underlying substrate, provides the necessary energy for the mass transport over large distances.

The phase obtained after overnight slow annealing to room temperature phase (o) in Fig. 4(b) (prepared at 120 K with $\theta = 1.315$ ML) is (1,3) of lower coverage ($\theta = 1.286$ ML) as shown in profile p of Fig. 4(b). The pattern is extremely sharp with the observed spots accounted for exclusively from the (1,3) phase and with instrumentally limited full widths at half maximum. Some Pb must have been removed from the system [most likely to steps or to form very few two-layer Pb(111) islands[24]] since the coverage of the (1,3) phase is lower (and the triangle height H is 7% which is larger than the height of phase o). It is extraordinary that a single (1,3) phase covers the surface over macroscopic distances which requires even higher coverage uniformity than when two DS phases are present.

The low-temperature transformation from a lower- to a higher-coverage phase according to the DS phase diagram is also seen with STM. Figure 5(a) shows a 13.5×18.5 nm^2 image with the surface prepared in the $\sqrt{7}\times\sqrt{3}$ phase. After depositing an amount of $\Delta\theta\sim0.07$ ML Fig. 5(b) shows a dramatic change of the surface morphology with the (2,5), i.e., (1,2,1,3), similar to the ones shown in profile k in Fig. 4(b), thus confirming the diffraction results that a high-quality DS can be prepared at low temperature.

IV. FINITE TEMPERATURE EFFECTS IN DS

We would like to address briefly the second question raised in the introduction, i.e., what is the role of the finite

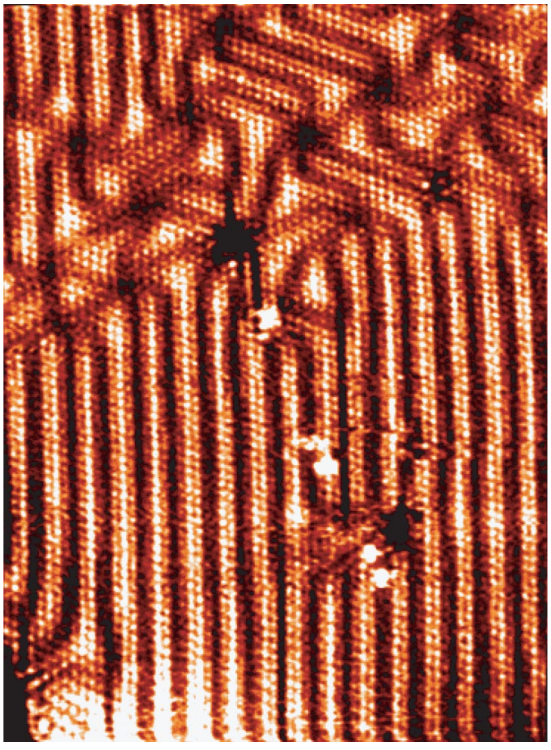

FIG. 8. STM image over a scale 38×50 nm^2 showing the coexistence of a 1D (1,2) phase with "HICC" phase as shown in the diffraction patterns of Fig. 6.

temperature in the formation of the DS phases since strictly speaking a DS is possible only at $T=0$? To answer the question we performed two types of experiments, first to deposit in a stepwise fashion (as in the experiment of Fig. 4) but at higher constant temperature $T>120$ K and, second, to anneal at constant θ to higher temperatures an initial DS phase formed at low temperature.

Figure 6 shows the results of the first type of experiment with Pb deposited at $T=169$ K and with larger coverage increments $\Delta\theta\sim0.01$ ML (than in the 120 K experiment). We observe again the same progression to $(n,1)$ phases with increasingly smaller n and higher coverage [the first stable phases resolved are (6,1) and (5,1) with $\theta=1.21$ ML. However, within the range $1.23<\theta<1.27$ ML instead of observing only 1D DS phases, a new phase of hexagonal symmetry, the ''HICA'' phase, is found to coexist with the (2,1) phase. A model of the ''HICA'' phase has been proposed in Ref. 25. It was identified as a commensurate phase of hexagonally arranged $\sqrt{3}\times\sqrt{3}$ triangular domains phase separated by light ''almost $\sqrt{7}\times\sqrt{3}$'' domain walls (this phase is slightly different from the ideal $\sqrt{7}\times\sqrt{3}$ phase because adjacent $[1\bar{1}2]$ rows have Pb atoms on $H3$ and $T4$ sites occupied instead of only $H3$ sites). Such ''HICA'' phase is easily distinguished with diffraction, because it gives rise to hexagonally arranged spots around $(\bar{1}/3,\bar{1}/3)$ rather than the triangular patterns of Fig. 3. A pair of spots is aligned along the $[11\bar{2}]$ direction resulting in the characteristic ''horizontal splitting'' described in earlier reflection high-energy electron diffraction and LEED studies.[26–28] The separation of the spot from the $(\bar{1}/3,\bar{1}/3)$ position can be used to deduce the domain size 4.7 nm for the HICA phase, consistent with the model proposed in Ref. 25 with STM. With further deposition of ~0.01 ML new types of ''HICA'' phases form (denoted as ''HICB'' and ''HICC'') with slightly higher coverage, i.e., larger $\sqrt{3}\times\sqrt{3}$ triangular domains, since the size of the observed hexagon decreases with increasing coverage. Details about the structure of these new ''HIC'' phases will be described in a future publication. For higher coverage $\theta>1.27$ ML 1D phases $(1,m)$ form, similar to the low-temperature $T=120$ K deposition experiments.

The ''HIC'' phases also form after heating to higher temperature a surface which is initially covered with 1D phase. The transition temperature T_c from a 1D to the ''HIC'' phase depends on the coverage of the 1D phase [T_c for the (1,1) phase with $\theta=1.25$ ML has the lowest $T_c\sim130$ K with all the other 1D phases undergoing the transition at higher T_c]. Typical results are shown in Fig. 7 with the (2,1) phase prepared initially on the surface at 136 K as evident from the size of the triangle height $H=26.6\%$ BZ. At 202 K the (2,1) coexists with the ''HICA'' phase. With annealing the pattern of the ''HICA'' phase reaches maximum intensity at 216 K but with further heating this phase gradually disorders, as seen from the lower intensity, until at 362 K only a (1×1) pattern is present. Cooling the surface back to 136 K restores the (2,1) but at slightly reduced intensity, indicating that possibly some Pb has diffused irreversibly to the steps. These thermally or coverage induced transformations of the (n,m) phases to the ''HIC'' phase and to what extent they are reversible or not, will be discussed in the future.

With coverage θ approaching 4/3 ML the thermally annealed phases give rise to the ''SIC'' phase, a phase consisting of $\sqrt{3}\times\sqrt{3}$ domains separated by meandering ''almost $\sqrt{7}\times\sqrt{3}$'' domain walls. The walls do not have the regular hexagonal arrangement as in the ''HIC'' phase (Fig. 8). They have shorter length per unit area than the hexagonally arranged domain walls, so higher coverage can be accommodated. No evidence for this ''SIC'' phase is found after deposition at low temperatures. The corresponding 1D scans for Fig. 4(b) show that the characteristic triangle height H continuously decreases and falls below the instrumental resolution which indicates the formation of large $\sqrt{3}\times\sqrt{3}$ domains with possibly extremely low $\sqrt{7}\times\sqrt{3}$ domain wall density which cannot be resolved in the diffraction patterns.

A different issue is related to the type of binding site the high-symmetry Pb atoms occupy in the unit cells of the generating phases. It has been observed in STM images and supported with first-principles calculations that the triangular domains of the HIC alternate between the Pb atoms occupying $H3$ vs $T4$ because these sites have approximately the same energy.[22] On the other hand, the structure of the ideal $\sqrt{7}\times\sqrt{3}$ phase ($\theta=6/5$ ML) has the high-symmetry Pb atoms only on $H3$ sites. It is interesting to ask whether the 1D (n,m) phases have only $H3$ sites occupied or at some coverage there is a transition with either $H3$ or $T4$ sites occupied). As mentioned before, we observe such a transition close to $\theta=1.25$ ML the coverage of the (1,1) phase (the coverage of the ''HICA'' phase although such a phase did not form at the low temperature deposition ~120 K of Fig. 4).

V. SUMMARY

In summary we have shown that DS phases in Pb/Si(111) in the range $6/5<\theta<4/3$ ML can be prepared after growth at low temperature without the need of thermal annealing. Only 1D phases are observed after stepwise deposition of small coverage amounts $\Delta\theta\sim0.006$ ML at 120 K and without the ''HIC'' phase which appears after thermal annealing or during deposition at higher temperature. Phases of larger periods (and smaller stability range) can be prepared at low temperatures rather than after thermal annealing. It is possible to cover macroscopic distances (0.5 mm the size of the incident electron beam) with predominantly two or even a single 1D phase by stepwise deposition of $\Delta\theta$. This unexpected formation of the DS at low temperature demonstrates that self-organization is possible, due to still unclear but very effective kinetic mechanisms.

ACKNOWLEDGMENTS

Ames Laboratory is operated by the U.S. Department of Energy by Iowa State University under Contract No. W-7405-Eng-82. This work was supported by the Director for Energy Research Office of Basic Energy Sciences.

*Corresponding author.
Electronic address: tringides@ameslab.gov

[1] L.D. Roelofs, in *Handbook of Surface Structure*, edited by W. Unertl (Elsevier, Amsterdam, 1997), Chap. 13.
[2] E. Bauer, in *Topics in Current Physics*, edited by W. Schommen and P. von Blanckenhagen (Springer-Verlag, Berlin, 1987).
[3] *Ordering in Two Dimensions*, edited by S.K. Sinha (North-Holland, New York, 1980).
[4] H. Taub, G. Torzo, H.J. Lauter, and S. Fain, *Phase Transitions in Surface Films 2* (Plenum, New York 1991).
[5] P. Bak, Rep. Prog. Phys. **45**, 587 (1982).
[6] V.L. Pokrovsky, A.L. Talapov, and P. Bak, in *Solitons*, edited by S.E. Trullinger, V.E. Zakharov, and V.L. Pokrovsky (North-Holland, Amsterdam, 1986), pp. 71–128.
[7] T.A. Kontorova and Ya.I. Frenkel, Zh. Eksp. Teor. Fiz. **8**, 89 (1938).
[8] S. Aubry, in *Solitons and Condensed Matter Physics*, edited by A.R. Bishop and T. Schneider (Springer-Verlag, Berlin, 1979), pp. 264–278.
[9] J. Hubbard, Phys. Rev. B **17**, 494 (1978).
[10] M.E. Fisher and W. Selke, Phys. Rev. Lett. **44**, 1502 (1980).
[11] P. Bak and R. Bruinsma, Phys. Rev. Lett. **49**, 249 (1982).
[12] M. Mandelbrot, *The Fractal Geometry of Nature* (Freeman, San Francisco, 1982).
[13] B.D. Krack, V. Ozolins, M. Asta, and I. Daruka, Phys. Rev. Lett. **88**, 186101 (2002).
[14] E.D. Tober, R.C.F. Farrow, R.F. Marks, G. Witte, K. Kalki, and D.D. Chambliss, Phys. Rev. Lett. **81**, 1897 (1998).
[15] P. Pieranski, P. Sotta, D. Rohe, and M. Imperor, Phys. Rev. Lett. **84**, 2409 (2000).
[16] D.F. McMorrow, D. Gibbs, and J. Bohr, in *Handbook on the Physics and Chemistry of Rare Earths*, edited by K.A. Gschneidner and L. Eyring (Elsevier, Amsterdam, 1999), p. 169.
[17] R.A. Cowley *et al.*, Phys. Rev. Lett. **66**, 1521 (1991); J.M. Tranquada *et al. ibid.* **73**, 1003 (1994).
[18] M. Hupalo, J. Schmalian, and M.C. Tringides, Phys. Rev. Lett. **90**, 216106 (2003).
[19] M. Nielsen, J. Als-Nielsen, J. Bohr, and J.P. McTague, Phys. Rev. Lett. **47**, 582 (1981).
[20] S.C. Fain, Jr., M.D. Chinn, and R.D. Diehl, Phys. Rev. B **21**, 4170 (1980).
[21] Ch. Kumpf, O. Bunk, J.H. Zeysing, M.M. Nielsen, R.I. Johnson, and R. Feidenhansl, Surf. Sci. **448**, L213 (2000).
[22] T.L. Chan, C. Zwang, M. Hupalo, M.C. Tringides, Z.Y. Lu, and K.M. Ho, Phys. Rev. B **68**, 045410 (2003).
[23] S. Stepanovsky, V. Yeh, M. Yakes, M. Hupalo, and M.C. Tringides (unpublished).
[24] M. Hupalo, V. Yeh, L. Berbil-Bautista, S. Kremmer, E. Abram, and M.C. Tringides, Phys. Rev. B **64**, 155307 (2001).
[25] M. Hupalo, T.L. Chan, C.Z. Wang, K.M. Ho, and M.C. Tringides, Phys. Rev. B **66**, 161410(R) (2002).
[26] L. Seehofer, G. Falkenberg, D. Daboul, and R.L. Johnson, Phys. Rev. B **51**, 13503 (1995).
[27] A. Petkova, J. Wollschlager, H.-L. Gunter, and M. Henzler, Surf. Sci. **471**, 11 (2001).
[28] K. Horikoshi, X. Tong, T. Nagao, and S. Hasegawa, Phys. Rev. B **60**, 13 287 (1999).